Research article

Jiangying Xia[a], Kang Xie[a], Jiajun Ma, Xianxian Chen, Yaxin Li, Jianxiang Wen, Jingjing Chen, Junxi Zhang, Sizhu Wu, Xusheng Cheng and Zhijia Hu*

The transition from incoherent to coherent random laser in defect waveguide based on organic/inorganic hybrid laser dye

https://doi.org/10.1515/nanoph-2018-0034
Received March 15, 2018; revised April 27, 2018; accepted May 7, 2018

Abstract: This paper systematically demonstrated a variety of experimental phenomena of random lasers (RLs) of N,N′-di-(3-(isobutyl polyhedral oligomeric silsesquioxanes)propyl) perylene diimide (DPP) organic/inorganic hybrid laser dye, which is composed of perylene diimide (PDI) as gain media and polyhedral oligomeric silsesquioxanes (POSS) as scattering media at a mole ratio of 1:2. In this work, we observe the transition from incoherent RL in the DPP-doped solutions and polymer membrane systems using dip-coating method to coherent RL in the polymer membrane system with defect waveguide using semi-polymerization (SP) coating method. Meanwhile, we found that the hybrid dye-DPP has a long lasing lifetime compared with the traditional laser dyes, which indicates that the POSS group can suppress the photo-bleaching effect to extend the working life of laser dyes.

Keywords: random laser; hybrid laser dye; nanoparticles; coherence.

1 Introduction

Since V. S. Letokhov theoretically proposed random lasers (RLs), it has been realized that the multiple light scattering in the disordered gain medium is a necessary condition for the forming of RLs [1, 2]. Due to low cost and easy fabrication [3, 4], RLs have drawn widespread attention for their potential applications and special properties – low spatial coherent and small size [5–8]. RLs have been investigated widely in different random systems doped with various gain media [9, 10], such as laser dyes [11–14], quantum dots [15–17], and luminescent nanocomposite materials [18]. However, RLs' applications are hindered due to luminescence quenching, which results in an increased non-radiative rate and a drastic decrease in the dye's radiative rate [19–21]. The enhancement of the thermal, optical, and mechanical properties of organic/inorganic hybrid matrices has led to a better laser action compared with the reported polar and nonpolar organic dyes [22–25]. Costela et al. have demonstrated that the RL photostability of organic/inorganic hybrid matrices is enhanced by incorporating silicon-containing polyhedral oligomeric silsesquioxanes (POSS) nanoparticles (NPs) into the structure of the organic monomers [25]. Cerdán et al. have indicated that the presence of POSS NPs results in additional amplified spontaneous emission and spectral narrowing [26]. The organic/inorganic hybrid laser dyes and POSS group have been applied in RL systems in the previous research [27–29]. Meanwhile, organic/inorganic hybrid laser dyes have been reported as active scattering medium including scatterer and gain medium,

[a]**Jiangying Xia and Kang Xie:** These authors contributed equally to this work.
***Corresponding author: Zhijia Hu,** School of Instrument Science and Opto-Electronics Engineering, Hefei University of Technology, Hefei, Anhui 230009, P.R. China; State Key Laboratory of Environment-Friendly Energy Materials, Southwest University of Science and Technology, Mianyang, Sichuan 621000, P.R. China; Aston Institute of Photonic Technologies, Aston University, Birmingham B4 7ET, UK; and Key Laboratory of Specialty Fiber Optics and Optical Access Networks, Shanghai University, Shanghai, 200072, P.R. China, e-mail: zhijiahu@hfut.edu.cn. http://orcid.org/0000-0002-8960-5318
Jiangying Xia, Kang Xie, Xianxian Chen, Yaxin Li, Jingjing Chen, Junxi Zhang and Sizhu Wu: School of Instrument Science and Opto-Electronics Engineering, Hefei University of Technology, Hefei, Anhui 230009, P.R. China
Jiajun Ma: State Key Laboratory of Environment-Friendly Energy Materials, Southwest University of Science and Technology, Mianyang, Sichuan 621000, P.R. China
Jianxiang Wen: Key Laboratory of Specialty Fiber Optics and Optical Access Networks, Shanghai University, Shanghai, 200072, P.R. China
Xusheng Cheng: Department of Computer and Information, Hefei University of Technology, Hefei, Anhui 230009, P.R. China

which are different from those dyes working only as gain medium [30, 31]. However, the random lasing features of the new organic/inorganic hybrid laser dyes DPP have not been researched systematically.

In this work, the laser characteristics of the DPP in different random systems have been systematically compared with traditional laser dyes for the first time. The incoherent laser is observed not only in DPP and CH_2Cl_2 solution in the cuvette but also in DPP-doped polystyrene (PS) film system. Meanwhile, to compare the random lasing properties of DPP in the solution systems, the spectra of DCP and pyrromethene 597 (PM597) mixed with POSS NPs solutions are also researched, and incoherent laser is observed in the DCP/POSS while coherent RL is found in PM597/POSS. In solid film systems, random lasing for the three kinds of dye-doped polystyrene films – DPP film (PSPP), DCP film (PSCP), and PM597 film (PSPM) – coated on the glass substrate has been researched using dip-coating method. The coherent RLs have been found in PSPM, while incoherent RLs have been found in PSPP and PSCP. Furthermore, we have fabricated defect polymer waveguide films using semi-polymerization (SP) coating film method; the styrene monomer was first pre-polymerized, was doped with DPP (DCP or PM597) as a viscous low molecular weight polystyrene, and then was coated on the glass substrate and continued to polymerize as polymer films, which are called LOPP, LOCP, and LOPM for the DPP-, DCP-, and PM597-doped polymer films, respectively. The defect polymer waveguide has resulted from two relatively parallel notches engraved on two opposing smaller cross-sections of the glass substrate. The coherent RLs have all been observed in the defect polymer film waveguide. In view of this, we observed the transition from incoherent RL to coherent RL. Meanwhile, for LOCP, the laser lifetime is short due to the photo-bleach effect. However, for LOPP, the advanced laser properties with stability, low threshold, and long lifetime have been obtained due to organic/inorganic hybrid effect, which proved that the POSS group can suppress the photo-bleaching effect in the RLs system.

2 Results and discussion

Figure 1A indicates the molecular structures of DPP, DCP POSS, and PM597. DPP is synthesized with two POSS NPs covalently attached to both side N atoms of perylene diimide (PDI), which is a type of fluorescent dye and could work as an active scatter [27]. Furthermore, DPP and DCP have been prepared according to the previous reports [32, 33].

We performed experiments on several scattering systems, which included passive scatterers embedded in laser dyes and active scatterers. Figure 1B–D shows the sample pictures in different systems. In the solution systems (Figure 1B), the samples are 5×10^{-4} M DPP (CHPP), 5×10^{-4} M DCP with 10^{-3} M POSS (Hybrid, Hattiesburg, USA) scattering NPs (CHCP), and 5×10^{-4} M PM597 (Exciton, USA) with 10^{-3} M POSS scattering NPs (CHPM) dissolved in the CH_2Cl_2 (SCR, Shanghai, China) solution. In the polymer film systems (Figure 1C), the random gain materials are dissolved in the polystyrene (PS, Aladdin, Shanghai, China) and CH_2Cl_2 solution, which are then dip-coated on the glass substrate and form the polymer films with a thickness of about 1 mm. The three kinds of dopant concentration in the PS film are 0.4 wt.% DPP (PSPP), 0.4 wt.% DCP (PSCP), and 0.4 wt.% PM597 (PSPM). The surface of these polymer films is scratched by knife to increase photonic multiple scattering. In the defect polymer waveguide system (Figure 1D), the styrene (SCR, Shanghai, China) monomer with dopants

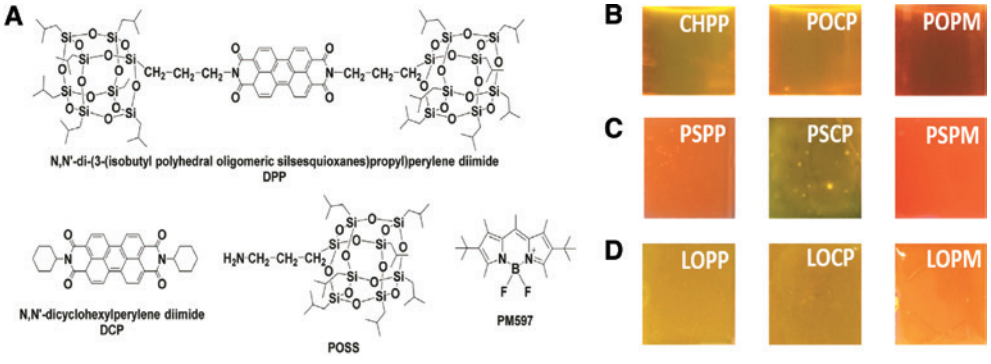

Figure 1: Materials structures and samples information.
The molecular structures of the DPP, DCP, POSS and PM597 (A). The solution samples pictures of CHPP, POCP and POPM (B); PSPP, PSCP and PSPM (C); LOPP, LOCP and LOPM (D).

is pre-polymerized to form low molecular weight viscous polymers at a temperature of 80°C for an hour, and then the pre-polymers with dopants are dip-coated on the glass substrate and continuously heated to obtain large molecular weight PS polymer films with a thickness of about 1 mm at 80°C. To induce effect in the polymer waveguide, two relatively parallel notches are engraved on two opposing ends of cross-sections of the glass substrate to increase the scattering. The three kinds of dopant concentration in the defect waveguide film also are 0.4 wt.% DPP, 0.4 wt.% DCP, and 0.4 wt.% PM597, respectively.

Figure 2 shows the measurement setup for the solution samples, the polymer film samples, and the waveguide film samples with defect. A Q-switched Nd:YAG laser (Q-smart 850, Quantel, France), which has an output wavelength of 532 nm with a round spots (pulse duration of 10 ns, repetition rate of 10 Hz, spot diameter of 100 nm), is used to end pump the different types of samples with convex lens 1 (D = 25 mm, f = 10 cm). Pump pulse energy and polarization are controlled by a Glan Prism group. A filter for 532 nm is placed behind the samples to filter the residual pump pulse. The emitted light is collected by a fiber spectrometer (QE65PRO, Ocean Optics, USA, resolution of ~0.4 nm, integration time of 100 ms). As shown in Figure 2A, the solution samples are pumped with 45° incidence angle, and the emitted light is collected by convex lens 2 (D = 25 mm, f = 5 cm) and received by using a spectrometer. In Figure 2B, the polymer film is pumped vertically by the pump laser and the transmitted emission spectrum is received by the spectrometer. For the defect polymer waveguide film (Figure 2C), the samples are pumped along the defect waveguide direction, and the emitted light from the notch on the other end is obtained by fiber spectrometer.

Figure 3 represents the absorption and fluorescence characterization of DPP, DCP, and PM597. It means that DPP and DCP samples in the CH_2Cl_2 solution contain a broad absorbance in 450 nm–550 nm with the main peak centered at 523.7 nm. The peak of PM597 is 527.1 nm. The emission peak wavelengths of DPP, DCP, and PM597 are 572 nm, 572 nm, and 562 nm, respectively. Figure 3C shows the fluorescence lifetime of DPP, DCP, and PM597, which are all ~9.2 ns. The fluorescence lifetime L_f can be formulated as $L_f = (T_2 - T_1)/e$, where L_f is the calculated value of a fluorescence lifetime and T_1 and T_2 are the time frames, as shown in Figure 3C. The characteristics of absorption and luminescence for DPP solutions sample indicate that the organic/inorganic hybrid dye-DPP can be a laser dye like the traditional laser dye of PM597, which can be applied in the dye laser field.

Figure 4 shows the random lasing features of the solution system. For DPP and DCP/POSS solution sample, we observed a broad spontaneous emission at low pumping energy (Figure 4B and Figure S1 in the Supplementary material). The narrow emission peaks of CHPP/CHDP can be observed located at 574.4/574.7 nm above the threshold at 800/364 μJ. The plots of integrated emission intensity and FWHM as a function of pumping energy for DPP and DCP/POSS sample are presented in Figure 4C and D, respectively. It can be clearly seen that there is an abrupt change at 830 μJ (364 μJ) for DPP (DCP/POSS) in the input-output energy plots, which are signature for the

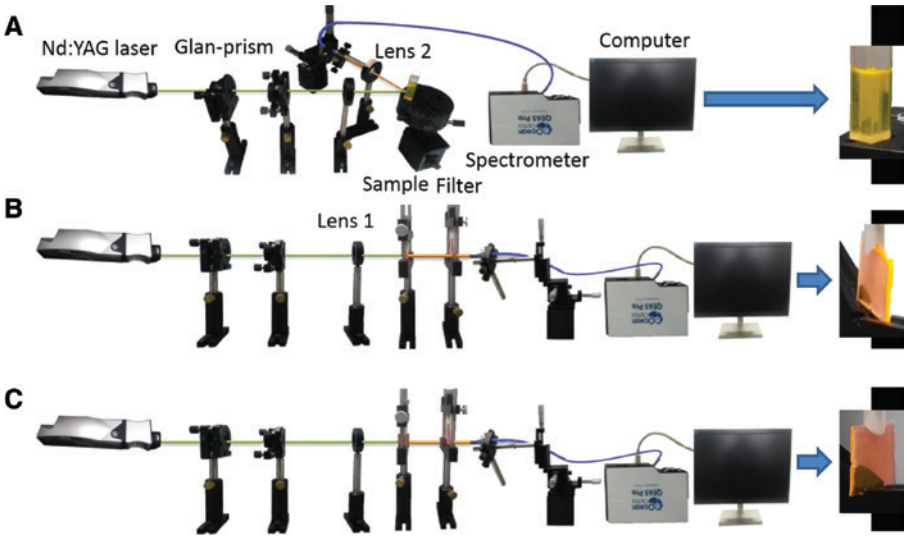

Figure 2: Measurement setup for different samples involved in the experiment.
The measurement setup for the solution samples (A), the dip-coating polymer film (B), and the defect polymer waveguide film (C).

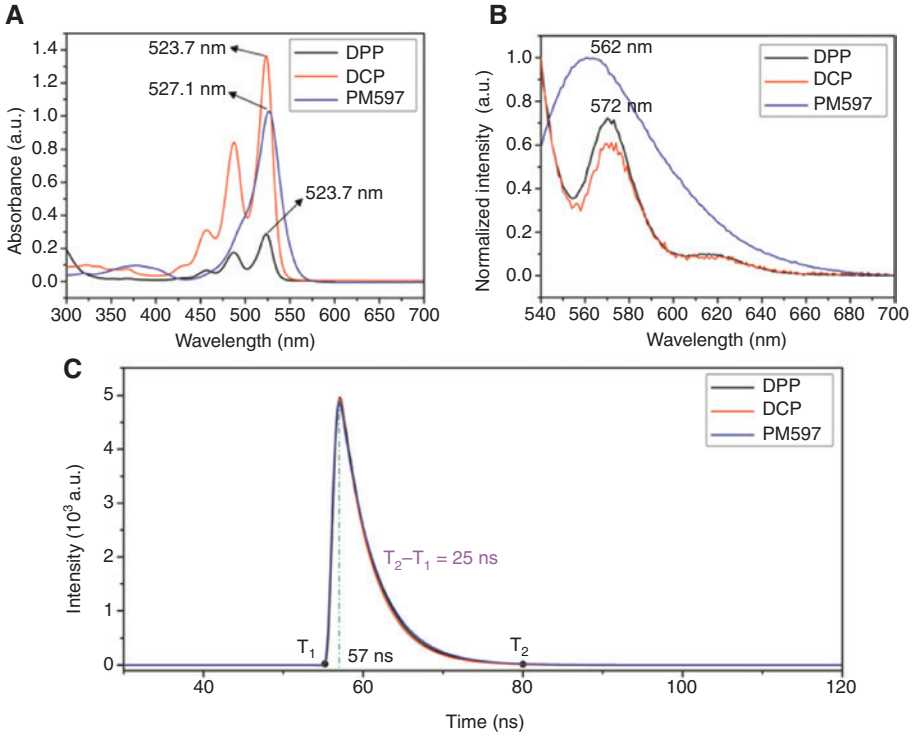

Figure 3: The optical properties of three laser dyes.
Absorption spectrum (A), emission spectrum (B) and fluorescence lifetime (C) of the DPP, DCP or PM597 in the CH_2Cl_2 solutions.

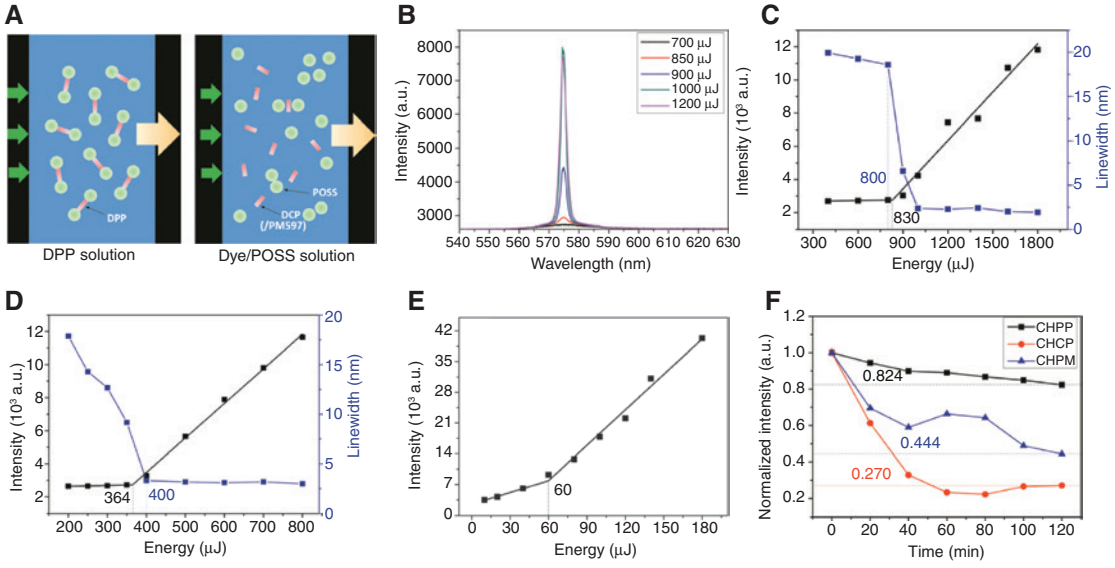

Figure 4: Random laser properties observed in the solution samples.
Excitation-emission of CHPP, CHCP, and CHPM (A); Emission spectra of CHPP with different pumping energy (B); integrated emission intensity and corresponding FWHM as function of pumping energy for CHPP (C); POCP (D); POPM (E). Random lasing lifetime for CHPP, CHCP and CHPM (F).

occurrence of lasing emission. And the FWHM sharply decreases to 1.92 nm (3 nm) from 19.94 nm (17.87 nm) around the turning points for DPP (DCP/POSS), which implies that incoherent RLs have been observed in DPP and DCP/POSS sample. This can be attributed to the fact that the scattering effect is so weak that the conditions forming Anderson localization cannot be reached to generate coherent RL for DPP and DCP/POSS sample. In the

PM597/POSS solution sample, there have been observed lasing spikes above the threshold and the main coherent random lasing spikes at 592.4 nm (Figure S2 in the Supplementary material), with the FWHM of ~0.33 nm, are measured under the pulsed laser excitation of 120 μJ, which indicates the different spectral characteristics between DPP/POSS and PM597/POSS. It can be observed in Figure 4E that the threshold of the PM597/POSS system is 60 μJ. The plot of the RLs lifetime of the solution samples is shown in Figure 4F. RL intensity decreases to 82.4%, 44.4%, and 27.0% for the CHPP, CHCP, and CHPM, respectively, after 72,000 time pulses pump due to photo-bleaching effect on pump energy of 900 μJ. It can be seen that the organic/inorganic hybrid laser dye-DPP has a long lasing lifetime compared with others, which can suppose that the POSS group can suppress the photo-bleaching effect to improve luminous stability in the organic/inorganic hybrid laser system.

We also have observed the luminous phenomenon in solid random systems in order to further study the emission characteristics of the organic/inorganic hybrid laser dye-DPP in the field of RLs. Figure 5A and Figures S3–S4 (see in the Supplementary material) show the emission spectra of DPP-, DCP-, and PM597-doped PS polymer film with different pulse pumping energy. At low energy illumination, the emission spectra are broad. However, narrow emission has occurred in the spectrogram after pumping energy is over the threshold. For the DPP (DCP)-doped PS polymer film, the narrowed peak can be observed in the wavelength of 577.9 nm (578.2 nm). As we can see from Figure 5B and C, there is non-linear variation between integrated intensity (FWHM) and pump energy. It can be seen that the threshold for the DPP- and DCP-doped PS polymer film is 78.46 μJ and 154.74 μJ, respectively. And the FWHM for DPP (DCP)-doped PS polymer films rapidly narrows to 4.16 nm (5.86 nm) from 24.99 nm (20.44 nm) over their threshold, which implies that incoherent RL has been found in the two samples. Similarly, this can be attributed to the fact that the scattering effect is so weak that the conditions forming Anderson localization cannot be reached to generate coherent RL for DPP and DCP. For PM597-doped PS polymer film, the broad emission spectra have been observed at low pump energy (<3.9 μJ) (Figure S3 in the Supplementary material). With the increase in pumping energy to ~9 μJ, multiple spikes in the emission spectra emerge, which demonstrate that coherent random lasing with ultra-low threshold has been observed. The main random lasing spikes at 587.07 nm, with the FWHM of ~0.33 nm, are observed under the pulsed laser excitation of 14 μJ. As shown in Figure 5D, it can be seen that there is a

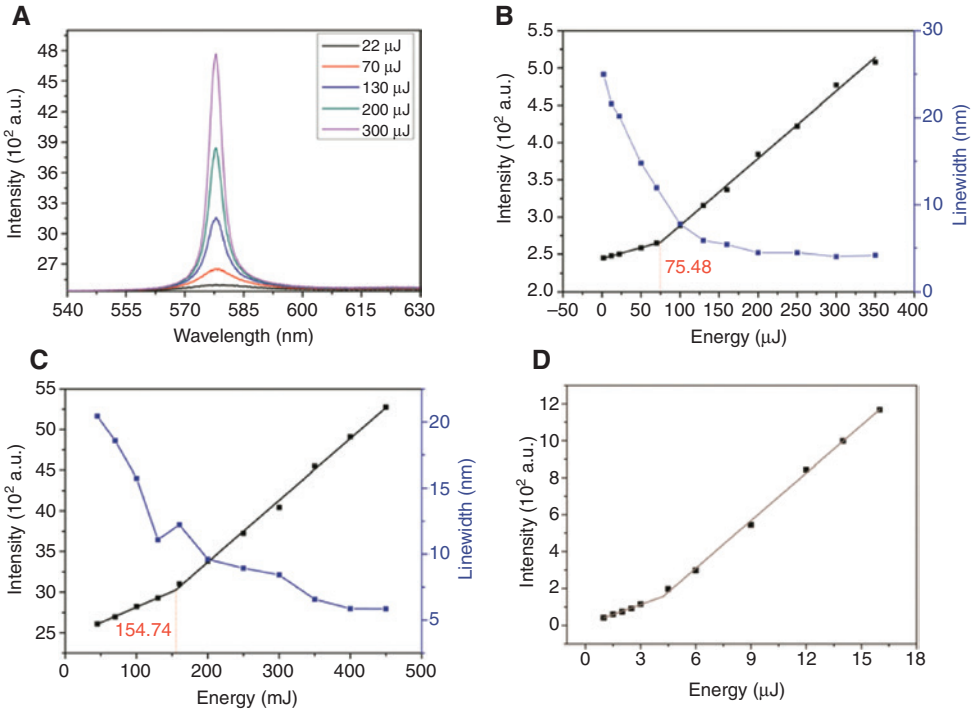

Figure 5: Random laser properties observed in the polymer films using dip-coating method.
Emission spectra of PSPP (A) with different pumping energy; integrated emission intensity and corresponding FWHM as function of pumping energy for PSPP (B), PSCP (C) and PSPM (D).

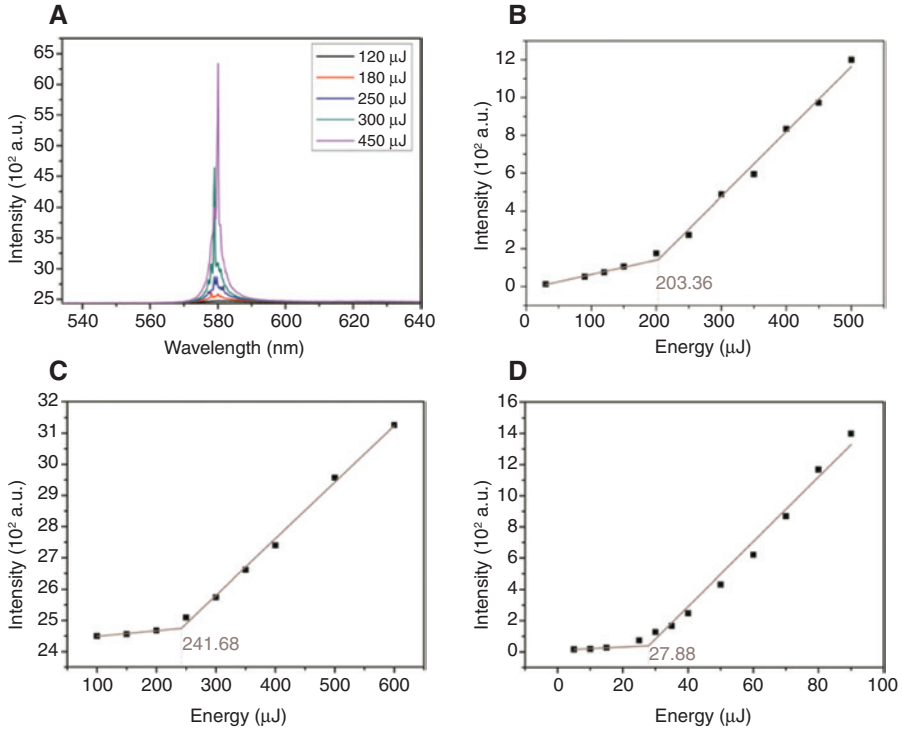

Figure 6: Random laser properties observed in the polymer films using semi-polymerization coating method.
Emission spectra of LOPP (A) with different pumping energy; integrated emission intensity and corresponding FWHM as function of pumping energy for LOPP (B), LOCP (C) and LOPM (D).

non-linear variation between input and output energy and the threshold can be determined at 9 μJ.

For DPP-doped samples, we found only incoherent RLs whether it is liquid or solid sample. The high-quality coherent RLs cannot be obtained with traditional coating and approaching methods. In order to derive high-quality coherent RLs, we introduced the SP coating method and defect into the PS waveguide film. Figure 6 shows the random lasing characteristic in the defect polymer waveguide film. The plot of emission spectra of DPP-, DCP-, and PM597-doped defect polymer waveguide film with different pumping energy is shown in Figure 6A and Figures S5–S6 in the Supplementary material. We observe a broad spontaneous emission at low pumping energy. When the pump energy is over the threshold, the multi-mode sharp peaks can be observed at the main peak wavelength of 579.5 nm, 580.5 nm, and 592.6 nm for the DPP-, DCP-, and PM597-doped defect polymer waveguide films, respectively, which are caused by the photonic multiple scattering in the defect polymer waveguide films. And we have observed the main sharp spikes at 580.1 nm, 580.4 nm, and 592.6 nm with the FWHM of ~0.42 nm, 0.18 nm, and 0.52 nm for DPP-, DCP-, and PM597-doped defect polymer waveguide films, respectively, which prove that coherent RLs are obtained in these samples. It suggests that there are Anderson localization effects that occur in the end of defect waveguide to generate coherent RL with the help of the waveguide confined effect. The non-linear variations between input and output energy are shown in Figure 6B–D. And the integrating range is 570.92 nm–598.75 nm for Figure 6B and C, while the integrating range is 577.95 nm–610.69 nm for Figure 6D. It can be seen that the threshold for DPP-, DCP-, and PM597-doped effect polymer waveguide film is 203.3 μJ, 241.68 μJ, and 27.88 μJ, respectively.

For coherent RL from the LOPP, Fourier transform of the emission spectrum of the LOPP has been analyzed at a pump energy of 450 μJ, as shown in Figure 7. In the Fourier transform of a laser cavity emission spectrum (separated by wave vector $K=2\pi/\lambda$, λ is the emission wavelength), there are spikes at P_m and these satisfy the following relationship:

$$P_m = mnL_c/\pi, \tag{1}$$

where m is the Fourier series number, n is the refractive index of the gain medium ($n_{ps}=1.6$), and L_c is the cavity path length.

Obviously, sharp emission peaks in the emission spectrum cause well-separated peaks in the Fourier transform.

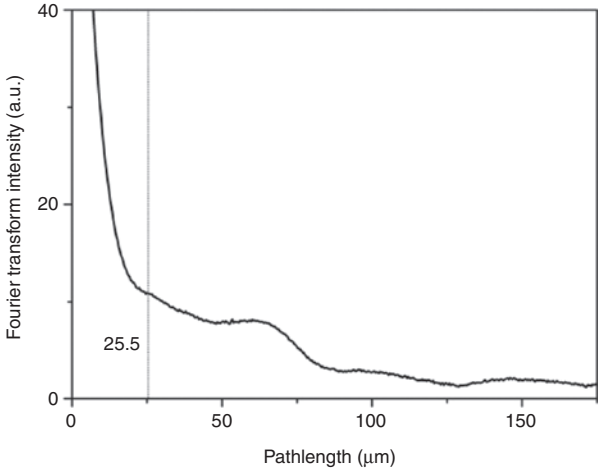

Figure 7: The Fourier transform corresponding to the emission spectrum of the LOPP of Figure 6(A) at a pump energy of 450 μJ.

As shown in Figure 7, the first peak ($m=1$) in the Fourier transform spectrum, we can draw $P_{m=1}=25.5$ μm and $L_c=50$ μm can be calculated from the formula.

Figure 8A shows the random lasing emission and far fieled images for the DPP-doped defect polymer waveguide film. And the transmission direction of light is the waveguide direction, which can be seen clearly in Figure 8A. It can be seen that there is strong lasing emission in the end of defect waveguide, which is the location of defect scattering. And this phenomenon proved our hypothesis – there is Anderson localization in the defect location. Figure 8B shows different spectra for changing the reception angle (0°~180° and surface), where *X* axis represents the direction of the waveguide, *Y* axis is perpendicular to the sample surface, and the reception angle is the angle between the *X* axis and the *Z* axis. It can be seen that random lasing spectra are different in the different angle, which demonstrates the multi-direction of RLs and the waveguide directionality. And we have observed that the largest intensity is at the reception angle of 90°, which can be attributed to the inhomogeneity of the notch on the defect polymer waveguide film.

In Figure 9A, we observed the lasing spectra from pulse to pulse pump for the LOPP at the same pump energy at ~350 μJ with the reception angle of 90°. For the peak wavelength of P_2 and P_4, the position of the random lasing peaks is relatively stable. However, there occurs an ~0.04-nm blue-shift relative to the wavelength of P_1 from 577.79 nm to 577.75 nm for the second time. Meanwhile, an ~0.13-nm red-shift relative to the wavelength of P_3 from 580.04 nm to 580.17 nm is observed in the third time. It is obvious that the peak intensities of P_1–P_4 are different for each time. As shown in Figure 9B, the path length of P_5 and P_7 is relatively stable, but an ~3.6-μm blue-shift from 59.94 μm to 56.34 μm and an ~5.83-μm red-shift from 59.94 μm to 65.77 μm relative to the path length of P_6 are observed in the third time and the fifth time, respectively. It can be seen that the position of the main random lasing peaks is relatively stable and some ignorable skewing, which is similar with that in our previous report [34].

Figure 10 shows the random lasing lifetime for the DPP-, DCP-, and PM597-doped effect polymer waveguide film at pump energy of 500 μJ. The RL intensity decreased to 81.5% and 5.9% for the DPP- and PM597-doped effect polymer waveguide film after 72,000 times pulses pump. However, the lasing spectra have disappeared after 6000 times pulses pump for DCP system. It can be seen that there is a strong photo-bleaching effect for the DCP and PM597 systems. But for the DPP system, the random lasing intensity with respect to the original intensity has a small decrement and is stabilized after 72,000 times pulse pump. In view of this, it can be proved that POSS group can suppress the photo-bleaching effect to improve

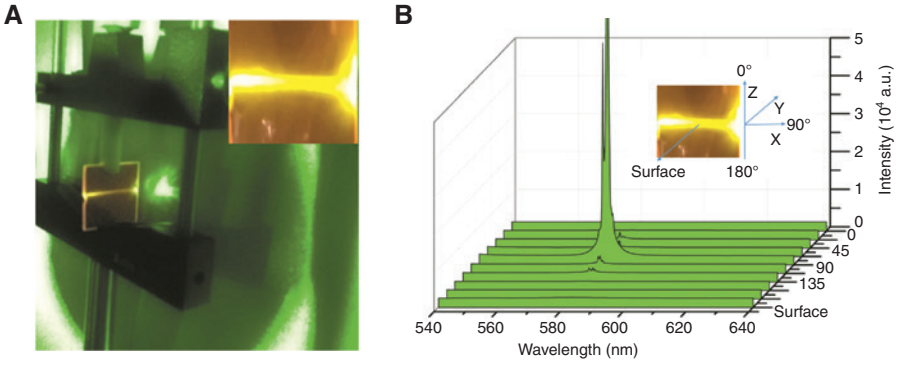

Figure 8: The formation mechanism and randomness of random Lasers observed in LOPP.
The random lasing emission and far filed images LOPP (A), the 3D waterfall of LOPP with different reception angle of spectrometer and reception diagram (B).

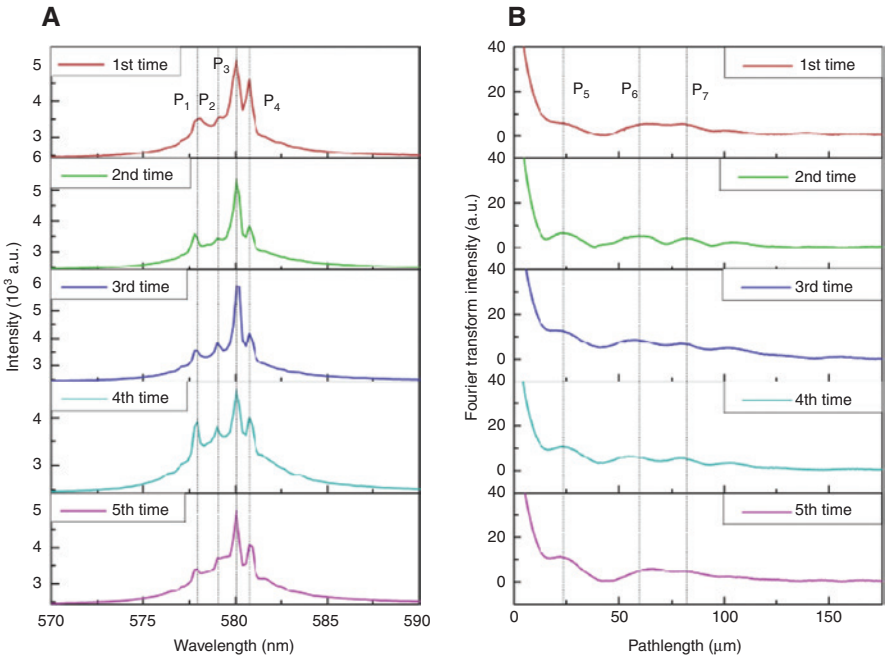

Figure 9: Spectral stability of random lasers observed in LOPP.
The waterfall of LOPP with different reception time at the same pump energy ~350 μJ (A). The Fourier transform corresponding to the emission spectrum of the LOPP with different reception time at the same pump energy ~350 μJ (B).

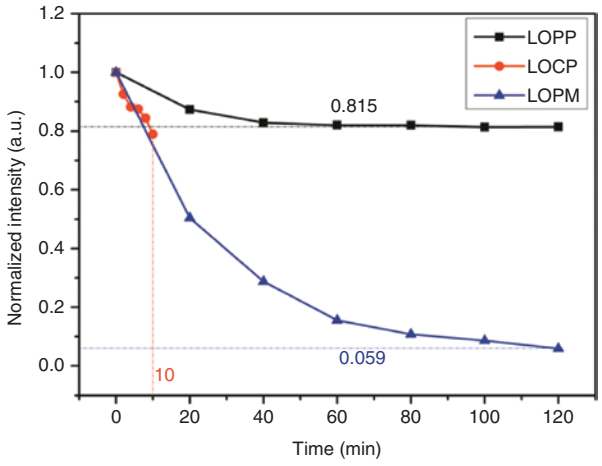

Figure 10: The normalized intensity of the main peak versus pump times for LOPP and LOPM.

luminous stability in the organic/inorganic hybrid laser system, which is also echoed with the solution system for DPP laser dye.

Table 1 shows the incoherent and coherent RLs in different dyes-doped random systems. Coherent RLs have been observed in the DPP-doped defect polymer waveguide film, while incoherent RLs have been observed in DPP-doped solution sample and traditional PF. For PM597-doped samples, coherent RLs can be observed in PS polymer film and defect polymer waveguide film. High-quality coherent

Table 1: Types of random laser in different random systems.[a]

Samples	Dopants		
	DPP	DCP	PM597
Solutions	INL	INL	INL
Traditional PF	INL	INL	CNL
Improved PF	CNL	CNL	CNL

[a]Solutions: liquid samples doped with DPP, DCP, or PM597; traditional PF, polymer films using dip-coating method; improved PF, polymer films using semi-polymerization coating method; INL, incoherent random laser; INL, coherent random laser.

RLs with the properties of good stability, low threshold, and strong light resistance in the DPP- and PM597-doped defect polymer waveguide film have been observed due to the combined effect of the waveguide confined and effective scattering effects. At this point, we observe the transition from the incoherent RLs in the DPP-doped solutions and PS polymer film to the coherent RLs in the DPP-doped defect polymer waveguide film.

3 Conclusion

To conclude, this paper systematically demonstrated the RLs for DPP, DCP, and PM597 dyes in the solutions,

polymer films using dip-coating method and defect polymer waveguide film using SP coating method. DPP can be considered an active scatterer working as gain medium and scattering medium, while DCP and PM597 only work as the gain medium. Incoherent RLs have been observed in solution sample and polymer film using dip-coating method doped with DPP. And coherent RLs have been found in defect polymer waveguide doped with DPP. We observed the transition from the incoherent RL in the DPP-doped solution samples and the polymer films using dip-coating method to the coherent RL in the defect polymer waveguide film. The phenomena can demonstrate that the generated Anderson localization to boost the coherent RL due to the waveguide confined and defect scattering effect of the end on the defect polymer waveguide film. Simultaneously, we have found that the SP coating method not only makes an interface between the polymer film and the glass substrate and becomes more tight but also simplifies complex embellishing processing for glass substrates. And we have found that POSS group can suppress the photo-bleaching effect to improve luminous stability in the organic/inorganic hybrid laser system.

Acknowledgment: The authors would like to thank the financial supports from the National Natural Science Foundation of China (11404087, 11574070, 11404086, 61501165), Fundamental Research Funds for the Central Universities (JZ2017HGTB0187, PA2017GDQT0024), China Postdoctoral Science Foundation (2015M571918, 2017T100442), the European Union's Horizon 2020 research and innovation program under the Marie Skłodowska-Curie grant agreement No 744817, STCSM, and the Natural Science Foundation of Anhui Province (1508085QA23).

References

[1] Letokhov VS. Stimulated emission of an ensemble of scattering particles with negative absorption. JETP Lett 1967;5:212–5.
[2] Aegerter CM, Maret G, Störzer M, Gross P. Observation of the critical regime near Anderson localization of light. Phys Rev Let 2006;96:063904.
[3] Polson RC, Vardeny ZV. Random lasing in human tissues. Appl Phys Lett 2004;85:1289–91.
[4] Redding B, Choma MA, Cao H. Speckle-free laser imaging using random laser illumination. Nat Photonics 2012;6:355–9.
[5] Wiersma DS. The smallest random laser. Nature 2000;406:132–3.
[6] Cao H, Xu JY, Seelig EW, Chang, RPH. Microlaser made of disordered media. Appl Phys Lett 2000;76:2997–9.
[7] Wiersma DS. The physics and applications of random lasers. Nat Phys 2008;4:359–67.
[8] Ling Y, Cao H, Burin AL, Ratner MA, Liu X, Chang RPH. Investigation of random lasers with resonant feedback. Phys Rev A 2001;64:063808.
[9] Gottardo S, Sapienza R, García PD, Blanco A, Wiersma DS, Lopez C. Resonance-driven random lasing. Nat Photonics 2008;2:429–32.
[10] Cao H. Review on latest developments in random lasers with coherent feedback. J Phys A-Math Gen 2005;39:10497–535.
[11] Yang L, Feng G, Yi J, Yao K, Deng G, Zhou S. Effective random laser action in Rhodamine 6G solution with Al nanoparticles. Appl Opt 2011;50:1816–21.
[12] Ye L, Yin Z, Zhao C, et al. Thermally tunable random laser in dye-doped liquid crystals. J M Optic 2013;60:1607–11.
[13] Ahmad M, Rahn MD, King TA. Singlet oxygen and dye-triplet-state quenching in solid-state dye lasers consisting of pyrromethene 567-doped poly(methyl methacrylate). Appl Opt 1999;38:6337–42.
[14] Hu Z, Xia J, Liang Y, et al. Tunable random polymer fiber laser. Opt Express 2017;25:18421.
[15] Chen Y, Herrnsdorf J, Guilhabert B, et al. Colloidal quantum dot random laser. Opt Express 2011;19:2996–3003.
[16] Hutchings M, O'Driscoll I, Smowton PM, Blood P. Fermi-dirac and random carrier distributions in quantum dot lasers. App Phys Lett 2014;104:031103.
[17] Augustine AK, Radhakrishnan P, Nampoori VPN, Kailasnath M. Enhanced random lasing from a colloidal CdSe quantum dot-Rh6G system. Laser Phys Lett 2015;12:025006.
[18] Ursaki VV, Tiginyanu IM, Sirbu L, Enachi M. Luminescent materials based on semiconductor compound templates for random laser applications. Phys Status Solidi 2010;6:1097–104.
[19] Dulkeith E, Morteani AC, Niedereichholz T, Klar TA, Feldmann J. Fluorescence quenching of dye molecules near gold nanoparticles: radiative and nonradiative effects. Phys Rev Lett 2002;89:203002.
[20] Bohren CF, Huffman DR. Absorption and scattering of light by small particles. Opt Laser Technol 1983;31:328.
[21] Ruan XL, Kaviany M. Enhanced nonradiative relaxation and photoluminescence quenching in random, doped nanocrystalline powders. J Appl Phys 2005;97:104331.
[22] García O, Sastre R, Garcíamoreno I, Martín V, Costela A. New laser hybrid materials based on POSS copolymers. J Phys Chem C 2008;112:14710–3.
[23] Sastre R, Martín V, Garrido L, et al. Dye-doped polyhedral oligomeric silsesquioxane (POSS)-modified polymeric matrices for highly efficient and photostable solid-state lasers. Adv Funct Mater 2009;19:3307–16.
[24] Angel C, Nmaculada GI, Luis C, Virginia M, Olga G, Roberto S. Dye-doped POSS solutions: random nanomaterials for laser emission. Adv Mater 2010;21:4163–6.
[25] Costela A, García-moreno I, Agua DD, García O, Sastre R. Highly photostable solid-state dye lasers based on silicon-modified organic matrices. J Appl Phys 2007;101:161–208.
[26] Cerdán L, Costela A, García-Moreno I, Garcia O, Sastre R. Laser emission from mirrorless waveguides based on photosensitized polymers incorporating POSS. Opt Express 2010;18:10247–56.
[27] Yin LC, Liang YY, Yu B, et al. Coherent random lasing from nanoscale aggregates of hybrid molecules by enhanced near zone scattering. RSC Adv 2016;6:85538–44.

[28] Yin L, Liang Y, Yu B, et al. Quantitative analysis of "$\Delta l = l_s - l_g$" to coherent random lasing in solution systems with a series of solvents ordered by refractive index. RSC Adv 2016;6: 98066–70.
[29] Hu ZJ, Zheng HJ, Wang L, et al. Random fiber laser of POSS solution-filled hollow optical fiber by end pumping. Opt Commun 2012;285:3967–70.
[30] Hu, ZJ, Zhang Q, Miao B, et al. Coherent random fiber laser based on nanoparticles scattering in the extremely weakly scattering regime. Phys Rev Lett 2012;109:253901.
[31] Luan F, Gu B, Gomes ASL, Yong KT, Wen S, Prasad PN. Lasing in nanocomposite random media. Nano Today 2015;10:168–92.
[32] Zhuang XD, Chen Y, Zhang B, Li Y, Qiao W. A highly soluble polyhedral oligomeric silsesquioxane end-capped perylenediimide dye. New J Chem 2010;34:1120–4.
[33] Che Y, Yang X, Balakrishnan K, Zuo J, Zang L. Highly polarized and self-waveguided emission from single-crystalline organic nanobelts. Chem Mater 2009;21:2930–4.
[34] Hu ZJ, Miao B, Wang TX, et al. Disordered microstructure polymer optical fiber for stabilized coherent random fiber laser. Opt Lett 2013;38:4644–7.

Supplemental Material: The online version of this article offers supplementary material (https://doi.org/10.1515/nanoph-2018-0034).